

# Theoretical study of potential high-pressure phases of TaON and a quaternary ZrTaO<sub>3</sub>N

J. E. Lowther

*DST/NRF Centre of Excellence in Strong Materials and School of Physics, University of the Witwatersrand, Johannesburg, South Africa*

(Received 17 October 2005; revised manuscript received 14 March 2006; published 17 April 2006)

Zirconia has a monoclinic ambient phase with several important phases formed under extreme conditions. TaON is an oxynitride material displaying similar characteristics to ZrO<sub>2</sub> in that it also has an ambient monoclinic phase. A theoretical study is carried out using the local density functional theory to investigate the properties of similar structural phases as those displayed in ZrO<sub>2</sub> for the system TaON. The intermediate structure ZrTaO<sub>3</sub>N is also investigated and the stability of these materials related to the parent phases ZrO<sub>2</sub> and TaON. Smooth trends are observed between ZrO<sub>2</sub> and TaON in the electronic properties with a steady change in compressibility. The elastic constants of high-pressure phases are also obtained strongly implying that the hardness increases between ZrO<sub>2</sub> and TaON.

DOI: 10.1103/PhysRevB.73.134110

PACS number(s): 61.72.Vv, 71.55.Eq

## I. INTRODUCTION

Of all the metal oxides, zirconia is the most studied now having an extensive range of industrial applications.<sup>1–3</sup> Several distinct phases of ZrO<sub>2</sub> have been observed and identified to date experimentally and the potential of the material to be a useful hard material is well known. Zirconia assumes a monoclinic<sup>4</sup> ( $P2_1/c$ ) or baddeleyite structure containing four ZrO<sub>2</sub> molecules per unit cell under ambient conditions. It transforms into a tetragonal form ( $P4_2/nmc$ ,  $Z=2$ ) at 1440 K (Ref. 5) and a cubic fluorite ( $Fm\bar{3}m$ ,  $Z=4$ ) form<sup>6</sup> around 2640 K and then finally melts at 2950 K. The ambient monoclinic structure is relatively soft<sup>7,8</sup> and as such affords little industrial application for a refractory usage but other structures such as the cubic or tetragonal structures do have important hardness properties and as such are very useful industrial materials. Cubic ZrO<sub>2</sub> is notably valued for its hardness and tetragonal ZrO<sub>2</sub> is used as a metastable phase often employed in a composite with other ceramics. Another much sought after phase of ZrO<sub>2</sub> is obtained after quenching from about 1000 °C and a pressure of about 15 GPa.<sup>9–13</sup> This phase of zirconia has an orthorhombic structure that is commonly called the cotunnite phase—and this is the phase with the largest coordination of O atoms. Following similar arguments relating to that of SiO<sub>2</sub> where the Si coordination affects the hardness of the structure, the cotunnite structure is considered as an important potential superhard phase of ZrO<sub>2</sub>.

Stabilization of the oxide materials is an annoying feature of metal oxide materials and in the cubic or tetragonal structures additional chemical impurities such as yttrium are often introduced.<sup>14–16</sup> While the exact nature of the stabilization mechanism is not well established to date,<sup>17</sup> it is generally thought that the effect of the additional impurity is to introduce O vacancies that lower the coordination about the Zr and thus revert to an effective or apparent coordination characteristic of the ambient monoclinic structure. It has also been suggested that the cotunnite structure may also be stabilized by the addition of oxides of Mg or Ca.<sup>18–20</sup>

Tantalum oxynitride, on the other hand, is a new ternary material that has not so far received much consideration as a

potentially hard material. It has recently been successfully synthesized<sup>21–23</sup> and a suggestion was made that it could be an efficient semiconductor pigment<sup>24</sup> or a photocatalyst.<sup>25</sup> It has a similar ambient phase as ZrO<sub>2</sub> (Ref. 26)—the monoclinic or baddeleyite structure—and with a very similar size in the crystal dimensions. The phase has received some theoretical analysis<sup>27–30</sup> where some properties of the material were confirmed and the potential of the material speculated.

Given the similarity of the ambient phases of the two materials—ZrO<sub>2</sub> and TaON—the possibility that combinations of such materials could form a quaternary structure of the form Ta<sub>3–x</sub>Zr<sub>x</sub>N<sub>5–x</sub>O<sub>x</sub> with  $0 < x < 0.66$  or Ta<sub>1–x</sub>Zr<sub>x</sub>N<sub>1–x</sub>O<sub>1+x</sub> with  $0 < x < 0.28$  has also recently been considered.<sup>24,31</sup> Mainly this is because of the potential application as an optoelectronic material and, as with the use of

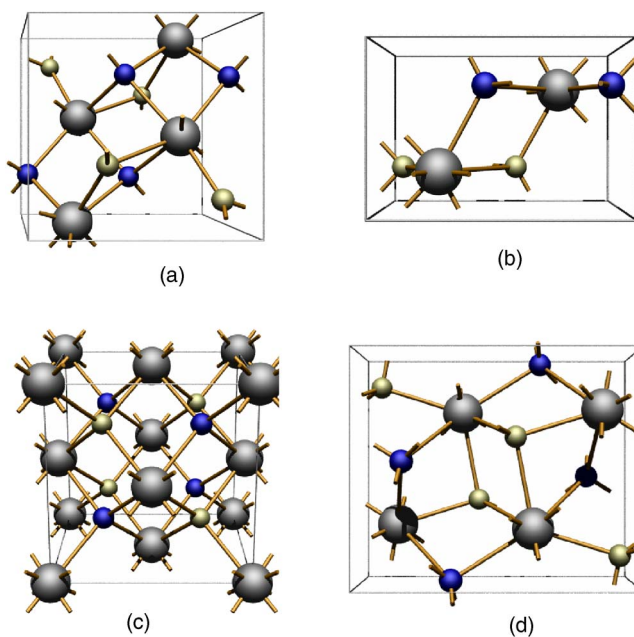


FIG. 1. (Color online) Crystal structure of some TaON phases. (a) monoclinic (baddeleyite), (b) tetragonal, (c) cubic, and (d) orthorhombic (cotunnite) structure.

TABLE I. Cell structure of  $\text{ZrO}_2$  and TaON. Experimental values (in parantheses) for  $\text{ZrO}_2$  are taken from Refs. 12 and 45 and for TaON from Ref. 27.

Phase	Lattice ( $\text{\AA}$ )	Wykoff coordinates	Lattice ( $\text{\AA}$ )	Wykoff coordinates
Baddeylite ( $P2_1/c$ )	$a=5.122(5.150)$	Zr 0.278,0.542,0.209	$a=4.925(4.9682)$	Ta 0.294,0.046,0.215
	$b=5.218(5.212)$	O 0.073,0.843,0.336	$b=5.001(5.0368)$	O 0.062,0.327,0.346
	$c=5.280(5.315)$	O 0.447,0.258,0.482	$c=5.146(5.1849)$	N 0.4397,0.756,0.481
	$\beta=99.94$		$\beta=99.93(99.602)$	
Modified fluorite ( $F\bar{4}3m$ )	$a=5.064(5.086)$		$a=4.827$	
Tetragonal ( $P4_2/mc$ )	$a=3.583(3.605)$	Zr 0.250,0.750,0.250	$a=3.476$	Ta 0.250, 0.750, 0.255
	$c=5.140(5.180)$	O 0.250,0.250,0.041	$c=5.101$	O 0.250, 0.250, 0.063
				N 0.750, 0.750, 0.434
Cotunnite ( $Pnma$ )	$a=5.553(5.741)$	Zr 0.245,0.750,0.617	$a=5.384$	Ta 0.251,0.750,0.628
	$b=3.299(3.246)$	O 0.358,0.750,0.929	$b=3.075$	O 0.364,0.750,0.933
	$c=6.472(6.341)$	O 0.028,0.250,0.834	$c=6.426$	N 0.032,0.250,0.837

TaON, from the point of view of using the material as a semiconductor pigment. The replacement of Zr ions by smaller Ta is probably counteracted by the simultaneous substitution of O ions by larger N ions, thus making the quaternary Zr-Ta-O-N structure quite feasible. As with TaON, the possibility that higher phases exist in the quaternary structure when the material is subject to extreme conditions has so far not been explored either theoretically or experimentally.

In this paper we examine the properties of the Zr-Ta-N-O system and especially the conditions that may be necessary for the formation of similar phases as that found in  $\text{ZrO}_2$ . A further motivation is to identify the properties of the TaON high-pressure structures and the potential properties of quaternary structures based on mixtures of  $\text{ZrO}_2$  and TaON.

The theoretical approach uses the density functional theory—namely the local density approximation (LDA)—as a way of treating the electron exchange and correlation, an approach that is now commonly used in analyzing systems similar to the one specified here. It is acknowledged that difficulties remain concerning an accurate description of the pseudopotentials needed especially for Zr, and as such the present calculations may be seen more in terms of a prediction of trends. We shall investigate properties of the most important phases, namely the ambient baddeylite phase with phases that may tentatively be formed from this phase under high-pressure conditions. Throughout, even within restrictions of the calculational approach, the aim is to see if there are trends in the alloy system and if important properties could be modified in the new ternary or quaternary systems.

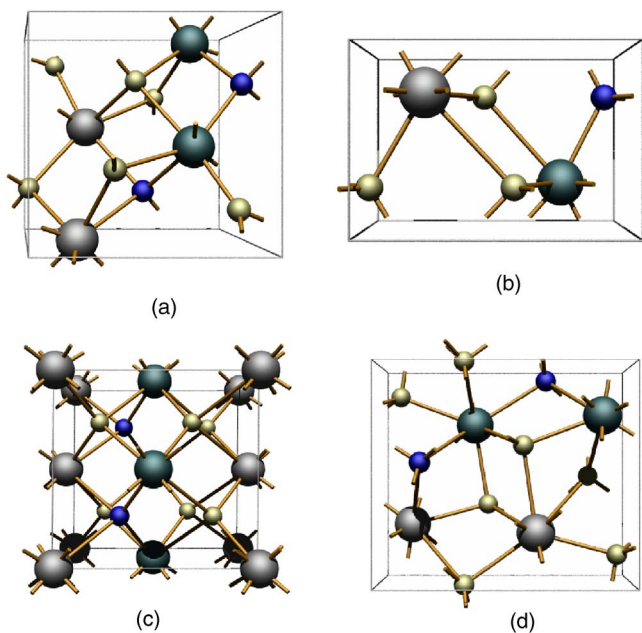


FIG. 2. (Color online) Crystal geometry of some  $\text{ZrTaO}_3\text{N}$  phases. (a) monoclinic, (b) derived from tetragonal, (c) derived from cubic, and (d) orthorhombic phases.

## II. COMPUTATIONAL

The computational approach employed uses projector augmented wave (PAW) pseudopotentials<sup>32</sup> within LDA as parametrized by Perdew and Zunger<sup>33</sup> and carried out

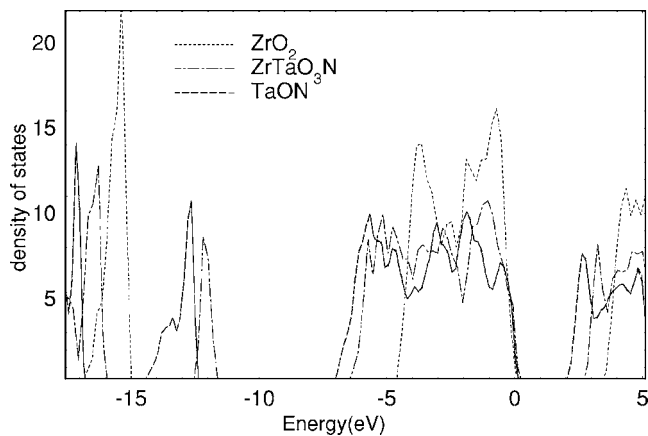


FIG. 3. Density of states of the monoclinic structure; the Fermi energy is at zero energy.

TABLE II. Cell structure of  $\text{ZrTaO}_3\text{N}$ . Experimental values (in parentheses) for  $\text{Zr}_{0.28}\text{Ta}_{0.72}\text{O}_{1.28}\text{N}_{0.72}$  from Ref. 24.

Phase	Lattice ( $\text{\AA}$ )		Wykoff coordinates
Monoclinic ( $P2_1$ )	$a=5.0158(5.008)$	Zr	0.285,0.035,0.214
	$b=5.0900(5.0723)$	Ta	0.287,0.445,0.713
	$c=5.2500(5.2171)$	O	0.083,0.353,0.100
	$\beta=99.07(99.576)$	O	0.944,0.689,0.406
		O	0.477,0.746,0.238
		N	0.555,0.231,0.288
“Near-tetragonal” ( $Pmm2$ )	$a=3.507$	Zr	0.000,0.000,0.242
	$b=3.535$	Ta	0.500,0.500,0.761
	$c=5.260$	O	0.000,0.500,0.043
		O	0.000,0.500,0.565
		O	0.500,0.000,0.453
		N	0.500,0.000,0.936
Orthorhombic ( $Pmm2_1$ )	$a=5.553$	Zr	0.000,0.488,0.118
	$b=3.299$	Ta	0.000,0.015,0.375
	$c=6.472$	O	0.000,0.392,0.429
		O	0.000,0.881,0.069
		O	0.000,0.257,0.840
		N	0.000,0.804,0.668

through a variable-cell option of the VASP electronic structure code.<sup>34</sup> A plane wave basis calculated on *at least* an  $8 \times 8 \times 8$  Monkhorst-Pack grid<sup>35</sup> has been employed to achieve convergence. LDA usually gives a better description of the cohesive properties and also the elastic constants and as the present calculation is to primarily identify the cohesive character, LDA has been used throughout. A full geometry optimization has been performed on each system with all atoms relaxing as the cell structure changed. As pointed out in earlier calculations<sup>7</sup> the Zr pseudopotential is especially sensitive to cutoff radii and for this reason a cutoff radius of 500 to 800 eV was used on at least  $8 \times 8 \times 8$  Monkhorst-Pack grid to obtain an energy convergence with PAW pseudopotentials.<sup>32</sup> This makes the calculations extremely computationally demanding but, as we shall see, the energy

differences between the various phases are extremely small thus requiring as large an accuracy as possible.

### A. Structural properties

As a starting point we have used the cell parameters and fractional atomic coordinates of  $\text{ZrO}_2$  for each of the various phases we have considered in the present work and in Table I we show the optimized calculated structural parameters both for  $\text{ZrO}_2$  and for TaON. In the ternary TaON systems the crystal structures are schematically represented in Fig. 1. As can be seen from Table I, the crystal dimensions of all the phases of TaON are not too far from the equivalent  $\text{ZrO}_2$  phases. However, there are subtle modifications of the relative energies and cohesive properties that we shall return to later. We note that the reduction in volume for each phase is as predicted recently by us<sup>30</sup> for the cotunnite phase as cal-

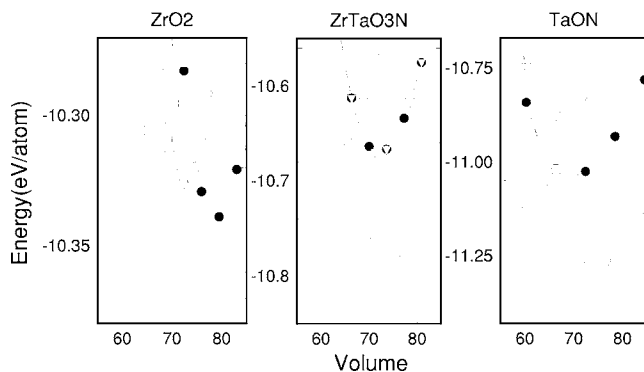


FIG. 4. Energy, volume variation of various derived phases of  $\text{ZrO}_2$ ;  $\circ$ , monoclinic;  $\bullet$ , tetragonal;  $\nabla$ , fluorite; and  $\square$ , orthorhombic derived phases.

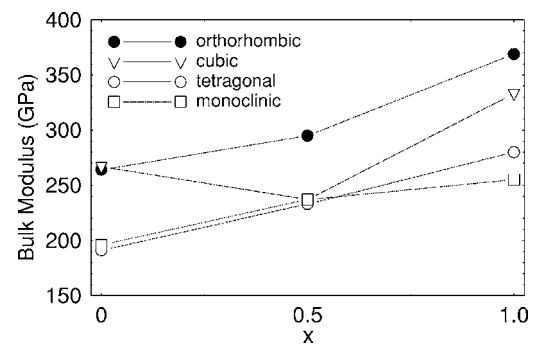


FIG. 5. Trend in the bulk modulus of  $\text{ZrO}_2$ ,  $\text{ZrTaO}_3\text{N}$  phases and TaON.

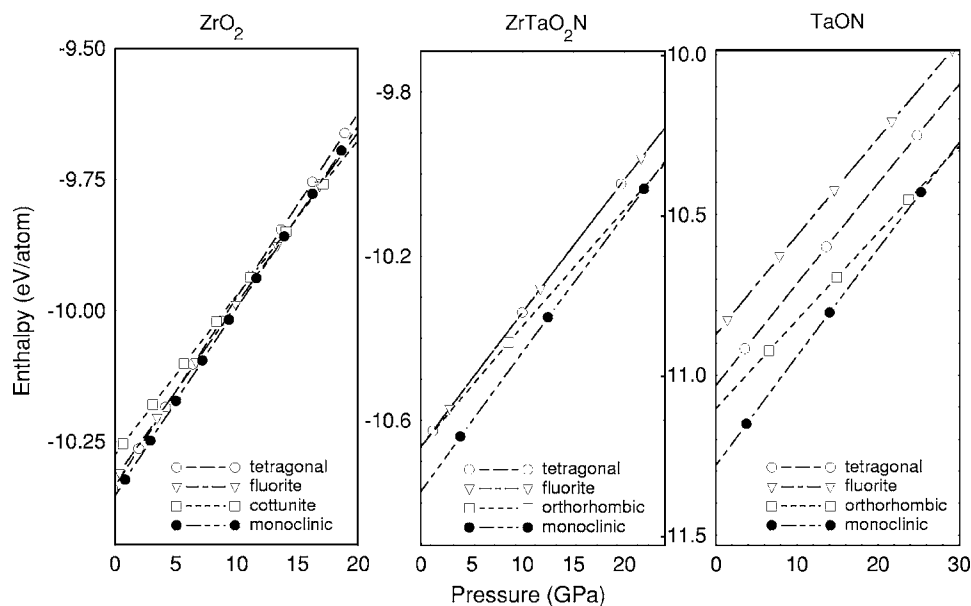


FIG. 6. Transition pressures of the various phases as calculated from the Birch equation of state.

culated using the LDA but with soft Troullier Martins potentials.

We then considered replacing equal amounts of  $ZrO_2$  and TaON together to give the quaternary alloy  $ZrTaO_3N$ . The crystal symmetries become subtly changed by this replacement and we give the calculated dimensions in Table II. The crystal structures are also shown schematically in Fig. 2; again there is a smooth trend in the volume—decreasing from  $ZrO_2$  to TaON.

Although we do not wish to go into great detail of the electronic properties of the material at this stage, we show in Fig. 3 the density of electronic states as calculated for the ambient phase. This phase has a baddeylite monoclinic structure having  $P2_1/c$  symmetry in both  $ZrO_2$  and TaON and for the quaternary  $Zr-Ta-O-N$  system of which  $ZrTaO_3N$  is considered here the space group symmetry is also mono-

clinic but with even lower symmetry now being simply  $P2_1c$ . Recently, Geunther *et al.*<sup>24</sup> have suggested that such a material will have the use as an optical pigment and found that substituting the energy band gap depends upon the relative concentration of nitrogen and oxygen atoms. Specifically the band gap increases in the material  $Ta_{1-x}Zr_xN_{1-x}O_{1+x}$  as the concentration as specified by  $x$  is increased. As shown from the density of states that have been deduced from the calculations in Fig. 3 the band gap does increase in going from TaON to  $ZrO_2$  as Geunther *et al.*<sup>24</sup> observe. Again it shows steady changes occurring from  $ZrO_2$  to TaON.

Now we examine the quaternary system  $ZrTaO_3N$ . As before we used as a starting point the crystal coordinates of the phases of  $ZrO_2$  for the crystal structures but, of course, in the quaternary structure  $ZrTaO_3N$ , there is now a lower symmetry caused because of different chemical substitutions. Of

TABLE III. Cell structure, total energy, relative stability, and some elastic properties of  $ZrO_2$ , TaON, and  $ZrTaO_3N$ .  $\Delta E_{tot}$  is the energy measured relative to the appropriate monoclinic phase. Previous results for  $\Delta E_{tot}$  (in parentheses) using ultrasoft pseudopotentials and the same computational procedure are taken from Ref. 7.

Phase	Space group	Material	$\Delta E_{tot}$ (eV/atom)	$V_{eq}$ ( $\text{\AA}^3$ )	$B$ (GPa)	$\Delta E_{stab}$ (eV)
Monoclinic ("baddeylite")	$P2_1/c$	TaON	0.000	10.37	280	
	$P2_1c$	$ZrTaO_3N$	0.000	11.04	233	0.043
	$P2_1/c$	$ZrO_2$	0.000	11.59	191	
Cubic	$F\bar{4}3m$	TaON	0.447	9.37	333	
	$Pmm2$	$ZrTaO_3N$	0.108	10.68	237	-0.087
	$F\bar{4}3m$	$ZrO_2$	0.031 (0.015)	10.82	267	
Tetragonal	$P4_2/mc$	TaON	0.250	10.27	255	
	$Pmm2$	$ZrTaO_3N$	0.107	10.68	237	0.016
	$P4_2/mc$	$ZrO_2$	0.019 (0.010)	11.00	196	
Orthorhombic ("cotunnite")	$Pnma$	TaON	0.178	8.88	369	
	$Pmn2_1$	$ZrTaO_3N$	0.111	9.42	295	0.080
	$Pnma$	$ZrO_2$	0.026 (0.018)	9.89	264	



TABLE IV. Elastic constants and effective isotropic elastic moduli (for calculational details see the Appendix) of different high-pressure phases. Experimental values for diamonds are  $B=442\text{--}433$ ,  $G=524\text{--}544$ ,  $E=1142\text{--}1164$ , and  $\nu=0.1$ . All moduli are in GPa. A low (high) value of  $B/G$  may be indicative of the material to be brittle (ductile). The smaller value of  $\nu$  may indicate the resistance of the material to shear.

		$c_{1,1}$	$c_{1,2}$	$c_{1,3}$	$c_{2,3}$	$c_{2,2}$	$c_{3,3}$	$c_{4,4}$	$c_{5,5}$	$c_{6,6}$	$B$	$G$	$B/G$	$E$	$\nu$
ZrO <sub>2</sub> tetragonal	This work	382	221	72			346		42	167	204	99	2.06	257	0.29
	Rigid ion potential (Ref. 46)	395	26	105			326		42	105	190	89		231	0.30
	Expt. (Ref. 47)	340	33	160			325	66		95	182	89		231	0.30
Fluorite	This work	499	111					63			240	115	2.08	298	0.29
	Rigid ion potential (Ref. 46)	455	64					63			194	105		266	0.27
	Expt. (Ref. 48)	417	82					47			194	116		290	0.25
Orthorhombic		474	164	201	149	348	314	68	114	132	254	112	2.26	293	0.31
TaON tetragonal		488	298	118			344	4		171	242	70	3.45	194	0.38
Fluorite		929	199					18			442	156	2.83	420	0.34
Orthorhombic		686	250	270	275	590	628	134	218	220	388	188	2.06	486	0.29

note were the starting “fluorite” and “tetragonal” systems. Despite having quite different structures in ZrO<sub>2</sub> and TaON, both the starting “fluorite” and “tetragonal” structures relaxed to the same equivalent phase that was orthorhombic and almost tetragonal. This in part comes about because of the tetragonal locations of ions in the starting nominal fluorite structure. It is interesting to note that, as discussed in previous calculations,<sup>7,36</sup> the fluorite to tetragonal phases transitions is a martensitic-displacive phase transition and strongly dependent on the asymmetric charge distribution about the metal atom sites. In the quaternary ZrTaO<sub>3</sub>N structure this asymmetry is clearly present, and it may be possible that alloying in this way could be a way that fluorite zirconia will transform to a new orthorhombic or even tetragonal structure.

### B. Cohesive properties and relative stability

Each structure considered in Tables I and II were subject to the uniform compression and the resulting energy-volume variations are shown in Fig. 4. In turn this variation was fitted to a Birch equation of state<sup>37</sup> from which an estimate of the bulk modulus can then be deduced through a least-squares fitting procedure. The equation of state parameters with the relative energies of phases relative to the ambient monoclinic phase are also shown in Table III. The trend in the bulk modulus is shown in Fig. 5.

Here, we are also considering the quaternary phase and we have to estimate the relative stability of this phase with respect to each of its separate constituent phases. A simple measure of the relative stability of the quaternary structure is defined—without any application of extreme conditions such as pressure or temperature—by the following expression:

$$\Delta E_{stab} = E_{tot}[\text{ZrTaO}_3\text{N}] - E_{tot}[\text{ZrO}_2] - E_{tot}[\text{TaON}].$$

The implication of this definition is that if  $\Delta E_{stab}$  is positive the two separate phases are immiscible while if  $\Delta E_{stab}$  is negative the phases are miscible. The values for  $\Delta E_{stab}$  are also contained in Table III. It is pointed out that extreme

conditions in themselves may affect conditions through which the two parent phases may mix.<sup>38</sup>

### C. Transition pressures

From the equation of state results expressed in Table III, a Enthalpy—pressure relationship can be established for each phase, where the pressure is deduced from the slope of the energy-volume relation. The enthalpy-pressure behavior is now shown for each structure in Fig. 6. As expected the transition pressures needed to reach the specific phases increase from ZrO<sub>2</sub> to TaON because relative energies between phases has also increased. We note that the predicted transition pressures are well within those that are available and 30 GPa predicted for cotunnite TaON formation on compression of the ambient baddeleyite phase is accessible in laboratory conditions.

### D. Elastic constants

Introducing effective isotropic, bulk, shear, or Young moduli as a combination of these elastic constants—as described in the Appendix—a further estimate of the physical behavior of the material can be made. Also an effective isotropic Poisson ratio can be deduced—this is considered as being a measurement of the material to resist shear—the smaller the value the more likely the material will resist shear. It has been suggested<sup>39</sup> that a ratio of  $B/G$  is related to the brittleness of the material with lower values suggesting that material is more brittle—Pugh<sup>39</sup> suggesting that when  $B/G < 1.75$  the material has ductile features when  $B/G > 1.75$  the material shows brittle character. The most important physical property is material hardness, while being a difficult concept to define<sup>40,41</sup> is generally related both to compressibility, as measured by the bulk modulus and to a shear modulus.

Using the *ab initio* approach it is possible to obtain all the elastic constants by an application of an appropriate deformation of the unit cell and, thereafter, some estimate of the appropriate effective isotropic moduli. For the high-pressure

TABLE V. Deformation strains used to calculate the elastic moduli of crystal structures.

Strain	$\Delta E/V$	
Tetragonal	$e_1=2x, e_2=e_3=-x$	$(5c_{1,1}-4c_{1,2}-2c_{1,3}+c_{3,3})x^2/2$
	$e_1=e_2=-x, e_3=2x$	$(c_{1,1}+c_{1,2}-4c_{1,3}+2c_{3,3})x^2$
	$e_1=e_2=x, e_3=-2x, e_6=2x$	$(c_{1,1}+c_{1,2}-4c_{1,3}+2c_{3,3}+2c_{6,6})x^2$
	$e_1=x$	$c_{1,1}x^2/2$
	$e_3=x$	$c_{3,3}x^2/2$
	$e_4=2x$	$2c_{4,4}x^2$
Cubic	$e_1=e_2=e_3=x$	$(c_{1,1}+2c_{1,2})x^2/3$
	$e_1=e_2=x, e_3=\{1/[(1+x)^2]\}$	$(c_{1,1}-c_{1,2})x^2/2$
	$e_3=x^2/(4-x^2), e_6=x$	$c_{4,4}x^2/2$
Orthorhombic	$e_1=x$	$c_{1,1}x^2/2$
	$e_2=x$	$c_{2,2}x^2/2$
	$e_3=x$	$c_{3,3}x^2/2$
	$e_2=e_3=-x, e_1=2x$	$(4c_{1,1}-4c_{1,2}-4c_{1,3}+c_{2,2}+2c_{2,3}+c_{3,3})x^2/2$
	$e_1=e_3=-x, e_2=2x$	$(c_{1,1}-4c_{1,2}+2c_{1,3}+4c_{2,2}-4c_{2,3}+c_{3,3})x^2/2$
	$e_1=e_2=-x, e_3=2x$	$(c_{1,1}+2c_{1,2}-4c_{1,3}+c_{2,2}-4c_{2,3}+4c_{3,3})x^2/2$
	$e_4=x$	$c_{4,4}x^2/2$
	$e_5=x$	$c_{5,5}x^2/2$
	$e_6=x$	$c_{6,6}x^2/2$

tetragonal, cubic, and orthorhombic structures, the appropriate cell deformations are described in the Appendix. The calculated energy changes were then fitted to a second rank polynomial to give the elastic constants. These values are now shown in Table IV together with the effective isotropic values. We point out that there is a fair agreement with the value of the bulk modulus as obtained from the Birch equation and the isotropic value as deduced from the elastic constants. Only the elastic constants for  $ZrO_2$  and TaON have been obtained in the present work as here the symmetry is well defined. However, we do see a clear trend—an increase from oxide to oxynitride. Thus we suggest from these results that the oxynitride will be harder than the oxide.

### III. DISCUSSION

The potential of  $ZrO_2$  to be a superhard material has now received much theoretical attention for almost a decade with various computational approaches being used in the hope that a fundamental understanding of the science of the material will lead to ways to control and thus stabilize high-pressure polytypes. In this paper we have extended these studies by examining the alloying of the material with another similarly behaving material TaON. TaON is a similar material to  $ZrO_2$  in that it has a monoclinic stable ambient phase that has a very similar structure to that of  $ZrO_2$ . We then investigated candidates for obtaining the important polytype structures in  $ZrO_2$  through an application of high

pressure also within the system TaON. Then we have considered the possible alloying of  $ZrO_2$  with TaON to give the material  $ZrTaO_3N$ .

First we have found a constant trend in that the bulk modulus of each structure increases in going from  $ZrO_2$  to TaON. This is so, but it is not the case for the fluorite structure that has a crystal structure that cannot exist in a crystal structure like  $ZrTaO_3N$ . Thus aside from fluorite we have deduced that TaON will enhance the properties of  $ZrO_2$ . An intermediate phase  $ZrTaO_3N$  has also been examined—however, the situation regarding the miscibilities and thus the relative stability of this phase relative to its parental counterparts is not as clear—some phases appear to exist as a chemical mix whereas others do not. However, there is always some uncertainty regarding quantifying the energy of the mixing and, for the ambient monoclinic phases, ample evidence now exists that the phases are chemically miscible.<sup>31</sup> Our calculations are for  $T=0$  K effectively and we found that the energy differences are quite small. Under synthesis con-

TABLE VI. Effective Voigt bulk and shear elastic constants.

Tetragonal	$B=\frac{1}{9}(2c_{1,1}+c_{3,3}+2c_{1,2}+4c_{1,3})$
	$G=\frac{1}{15}(2c_{1,1}+c_{3,3}-c_{1,2}-2c_{1,3}+6c_{4,4}+3c_{6,6})$
Cubic	$B=\frac{1}{3}(c_{1,1}+2c_{1,2})$
	$G=\frac{1}{5}(c_{1,1}-c_{1,2}+3c_{4,4})$
Orthorhombic	$B=\frac{1}{9}(c_{1,1}+c_{2,2}+c_{3,3}+2c_{1,2}+2c_{1,3}+2c_{2,3})$
	$G=\frac{1}{15}(c_{1,1}+c_{2,2}+c_{3,3}-c_{1,2}-c_{1,3}-c_{2,3}+3c_{4,4}+3c_{5,5}+3c_{6,6})$

ditions of the high pressure and temperature it would not be unexpected that the quaternary structures are formed.

One especially significant feature that has emerged is that there are marked differences in energy between the  $ZrO_2$  and the TaON phases and this, in turn, would affect the synthesis pressures needed to attain the various phases and even the possibility of different synthesis routes to a cotunnite structure. We have suggested that cotunnite TaON may have several properties that are superior to  $ZrO_2$ , and could be formed from a modest high-pressure treatment of the ambient monoclinic structure. We also presented evidence strongly suggesting that phases of TaON could be harder than  $ZrO_2$ .

#### ACKNOWLEDGMENT

This work has been supported by the N.R.F (S.A.)

#### APPENDIX

The calculation of elastic constants at an *ab initio* level has been the subject of several discussions.<sup>42–44</sup> By placing a specific strain on the crystal structure and then measuring the change in energy as a function of the deformation as specified by a dimensionless parameter  $x$ , the elastic moduli can be deduced for a specific system. In general, this strain can be described by the matrix

$$e = \begin{pmatrix} e_1 & e_6/2 & e_5/2 \\ e_6/2 & e_2 & e_4/2 \\ e_5/2 & e_4/2 & e_3 \end{pmatrix}$$

so that the calculated change in the energy variation with the deformation is obtained approximately as

$$\frac{\Delta E}{V} = f(e)x^2,$$

where  $f(e)$  is the specific stress having a form that is listed in Table V for the tetragonal, cubic and orthorhombic structures:

From the elastic constants an effective isotropic Voigt bulk and shear modulus can further be obtained using the expressions that are now given in Table VI.

Finally the bulk and shear modulus can be used to obtain an effective Young's modulus and Poisson ratio using the following expressions:

$$E = \frac{9BG}{3B + G},$$

$$\nu = \frac{(3B - 2G)}{2(3B + G)}.$$

- 
- <sup>1</sup>S. Desgreniers and K. Lagarec, Phys. Rev. B **59**, 8467 (1999).  
<sup>2</sup>J. M. Leger, P. E. Tomaszewski, A. Atouf, and A. S. Pereira, Phys. Rev. B **47**, 14075 (1993).  
<sup>3</sup>J. E. Lowther, MRS Bull. **28**, 189 (2003).  
<sup>4</sup>J. D. McCullough and K. N. Trueblood, Acta Crystallogr. **12**, 507 (1959).  
<sup>5</sup>P. Aldebert and J. P. Traverse, J. Am. Ceram. Soc. **68**, 34 (1985).  
<sup>6</sup>D. K. Smith and C. F. Cline, J. Am. Ceram. Soc. **45**, 249 (1962).  
<sup>7</sup>G. Jomard, T. Petit, A. Pasturel, A. L. Magaud, G. Kresse, and J. Hafner, Phys. Rev. B **59**, 4044 (1999).  
<sup>8</sup>J. E. Lowther, J. K. Dewhurst, J. M. Leger, and J. Haines, Phys. Rev. B **60**, 14485 (1999).  
<sup>9</sup>L. G. Liu, Earth Planet. Sci. Lett. **44**, 390 (1979).  
<sup>10</sup>S. Block, J. A. H. da Jornada, and G. J. Piermarini, J. Am. Ceram. Soc. **68**, 497 (1985).  
<sup>11</sup>Lin-Gun Liu, J. Phys. Chem. Solids **41**, 331 (1980).  
<sup>12</sup>J. M. Leger, J. Haines, and A. Atouf, J. Am. Ceram. Soc. **78**, 445 (1995).  
<sup>13</sup>L. C. Ming and M. H. Manghnani, in *Solid State Physics Under Pressure*, edited by S. Minomura (KTK Science, Tokyo, 1985), p. 135.  
<sup>14</sup>G. Stapper, M. Bernasconi, N. Nicoloso, and M. Parrinello, Phys. Rev. B **59**, 797 (2000).  
<sup>15</sup>A. S. Foster, V. B. Sulimov, F. Lopez Gejo, A. L. Shluger, and R. M. Nieminen, Phys. Rev. B **64**, 224108 (2002).  
<sup>16</sup>S. Ostanin, A. J. Craven, D. W. McComb, D. Vlachos, A. Alavi, A. T. Paxton, and M. W. Finnis, Phys. Rev. B **65**, 224109 (2002).  
<sup>17</sup>D. Simeone, G. Baldinozzi, D. Gosset, M. Dutheil, A. Bulou, and T. Hansen, Phys. Rev. B **67**, 064111 (2003).  
<sup>18</sup>O. Ohtaka, S. Kume, and E. Ito, J. Am. Ceram. Soc. **71**, C448 (1988).  
<sup>19</sup>S. R. U. Dev, L. C. Ming, and M. H. Manghnani, J. Am. Ceram. Soc. **70**, C218 (1987).  
<sup>20</sup>H. Fukui, T. Kunisada, T. Fujisawa, K. Funakoshi, W. Utsumi, T. Irifune, K. Kuroda, O. Ohtaka, and T. Kikegawa, Phys. Rev. B **63**, 174108 (2001).  
<sup>21</sup>E. Orhan, F. Tessier, and R. Marchand, SIAM (Soc. Ind. Appl. Math.) J. Sci. Stat. Comput. **4**, 1071 (2002).  
<sup>22</sup>W. J. Chun, A. Ishikawa, H. Fujisawa, T. Takata, J. N. Kondo, M. Hara, M. Kawai, Y. Matsumoto, and K. Domen, J. Phys. Chem. B **107**, 1798 (2003).  
<sup>23</sup>S. J. Clarke, K. A. Hardstone, C. W. Michie, and M. J. Rosseinsky, Chem. Mater. **14**, 2664 (2002).  
<sup>24</sup>E. Guenther and M. Jansen, MRS Bull. **36**, 1399 (2001).  
<sup>25</sup>Tsuyoshi Takata Junko, N. Kondo, Michikazu Hara, Hisayoshi Kobayashib, Go Hitoki, and Kazunari Domen, Chem. Commun. (Cambridge) **2002**, 1698 (2002).  
<sup>26</sup>O. Merdrignac-Conane, M. Guilloux-Viry, M. Kerlau, and A. Perin, SIAM (Soc. Ind. Appl. Math.) J. Sci. Stat. Comput. **6**, 101 (2004).  
<sup>27</sup>C. M. Fang, E. Orhan, G. A. de Wijs, H. T. Hintzen, R. A. de Groot, R. Marchand, J. Y. Saillard, and G. de With, J. Mater. Chem. **11**, 1248 (2001).  
<sup>28</sup>M. W. Lumey and R. Dronskowski, Z. Anorg. Allg. Chem. **629**, 2173 (2003).  
<sup>29</sup>M. W. Lumey and R. Dronskowski, Z. Anorg. Allg. Chem. **631**, 887 (2005).

- <sup>30</sup>J. E. Lowther, Phys. Rev. B **72**, 172105 (2005).
- <sup>31</sup>J. Grins, P. O. Kall, and G. Svensson, J. Mater. Chem. **4**, 1293 (1994).
- <sup>32</sup>G. Kresse and D. Joubert, Phys. Rev. B **59**, 1758 (1999).
- <sup>33</sup>J. P. Perdew and A. Zunger, Phys. Rev. B **23**, 5048 (1981).
- <sup>34</sup>G. Kresse and J. Hafner, Phys. Rev. B **47**, 558 (1993).
- <sup>35</sup>H. J. Monkhorst and J. D. Pack, Phys. Rev. B **13**, 5188 (1976).
- <sup>36</sup>H. J. F. Jansen, Phys. Rev. B **43**, 7267 (1991).
- <sup>37</sup>F. Birch, Phys. Rev. **71**, 809 (1947).
- <sup>38</sup>J. E. Lowther, J. Phys. Chem. Solids **66**, 1064 (2005).
- <sup>39</sup>S. F. Pugh, Philos. Mag. **45**, 823 (1954).
- <sup>40</sup>F. M. Gao, J. L. He, E. D. Wu, S. M. Liu, D. L. Yu, D. C. Li, S. Y. Zhang, and Y. J. Tian, Phys. Rev. Lett. **91**, 015502 (2003).
- <sup>41</sup>A. G. Lyapin, W. Brazhkin, and R. J. Hemley, Philos. Mag. A **82**, 231 (2002).
- <sup>42</sup>M. J. Mehl, B. M. Klein, and D. M. Papaconstantantopoulos, *First Principles Calculations of Elastic Properties of Metals, Intermetallic Compounds: Principles and Practice* Vol. 1 (John Wiley and Sons, London, 1993).
- <sup>43</sup>P. Ravindran, Lars Fast, P. A. Korzhavyi, B. Johansson, J. Wills, and O. Eriksson, J. Appl. Phys. **84**, 4891 (1998).
- <sup>44</sup>O. Beckstein (unpublished).
- <sup>45</sup>C. J. Howard, E. H. Kisi, and O. Ohtaka, J. Am. Ceram. Soc. **74**, 2321 (1991).
- <sup>46</sup>A. P. Mirgorodsky, M. B. Smirnov, and P. E. Quintard, Phys. Rev. B **55**, 19 (1997).
- <sup>47</sup>S.-K. Chan, Y. Fang, M. Grimsdithch, M. Z. Li, V. Nevitt, W. M. Robertson, and E. S. Zouboulis, J. Am. Ceram. Soc. **74**, 1742 (1991).
- <sup>48</sup>H. M. Kandil, J. D. Greiner, and J. F. Smith, J. Am. Ceram. Soc. **67**, 341 (1984).